Evolution characteristics of overburden structure and stress in strong mining of the deep coal seam: a case study

Junpeng Zou[1], Man Wang[2], Lu Bai[1]* and Chongwei Yan[3]

[1]State Key Laboratory of Water Resource Protection and Utilization in Coal Mining, Beijing, China, [2]College of Information Engineering, Wuhan Business University, Wuhan, China, [3]Faculty of Engineering, China University of Geosciences, Wuhan, China

As coal resources are gradually being extracted at depth, the overlying strata movement behavior and stress environment become complex and violent, leading to the frequent triggering of strong dynamic hazards. To promote the productivity and effectiveness of mining activities, this paper investigated the evolution characteristics of overburden structure and stress in deep mining by using theoretical analysis, on-site monitoring, and numerical simulation. Based on key strata theory, key layers were determined, and how their movement states have a controlling effect on surface subsidence was analyzed. The evolution process of the overburden spatial structure in deep mining was revealed, which was consistent with the "O-X" type structure. The surrounding rock stress at the working face has gone through three stages, violent change, slow increase, and fluctuant increase, and strong strata behaviors appear because of the fracture and collapse of key layers. The goaf will have a significant effect on the structure, stress, and deformation of the overlying rock, which results in a larger deformation of the surrounding rock within the vicinity. The narrow coal pillar fails to maintain the stability of the overburden structure when the stress exceeds the bearing capacity. The deformation law of the surrounding rock at the roadway was studied, concluding that the existence of the goaf leads to a further increase in deformation.

KEYWORDS

overburden structure, surrounding rock stress, key layers, "O-X" type structure, surface subsidence

1 Introduction

The extraction conditions and geological environment of deep mines have become increasingly complex as the mining of coal resources is gradually proceeding to the deep zone. Mine tremors, rock bursts, large deformation roadways, and other dynamic hazards are frequently triggered because the deep rock mass is characterized by a high temperature, high *in situ* stress, and high gas pressure (Xie and Gao, 2019; Xia and Yao, 2021; Xie and Li, 2021). It is essential to reveal the evolution characteristics of overburden structure and stress in deep mines to protect the productivity and effectiveness of mining activities.

The dynamic process of deep mining is essentially the coupling action of the surrounding rock stress, overlying strata movement, and gradual compaction of the collapsed rock blocks. The mining stress field, the stress distribution state after the repartitioning of overburden stress as a result of the excavation of the working face, breaks the equilibrium of the initial

stress field in rock (Guo and Yuvan, 2012; Dou and He, 2014; Ma and Westman, 2020; Zhou and Zhu, 2022; Wu and Zou, 2023; Zhang and Zou, 2023). The stress and deformation of rock mass show a significant dynamic evolution in the temporal and spatial dimensions influenced by mining stress and crustal stress. Scholars have investigated the structural and stress evolution characteristics of overlying rock strata under strong mining using theoretical analysis, field monitoring, numerical simulation, and model testing (Hatherly, 2013; He and Dou, 2015; Jian, 2017; Wang and Ma, 2018; Kuang and Li, 2019; Jiao and Wu, 2021). Based on key strata theory, thick and hard rock strata (THRS) play an important role in controlling overlying rock strata movement (Wu et al., 1997; Qian et al., 2000; Lu and Gong, 2019). Xu and Fu, (2019) analyzed the stress, energy, and size characteristics of dynamic hard strata failure and concluded that it has an obvious effect on dynamic hazards. Using numerical simulation, the effect of the fracture and movement of THRS on the pressure of coal-rock mass was studied by Yu and Zuo, (2022). The stress and fracture evolution laws of the ultra-thick hard roof have been summarized by Ju and Xiao, (2018) and are regarded as the brittle fracture for roof failure.

The strata behaviors in the stope are closely connected with the deformation and fracture characteristics of the THRS and the stability of the overburden structure in extraction (Guo and Yuvan, 2012; Ju and Xu, 2013; Mu and Liu, 2019; Mondal and Roy, 2020). THRS results in the increasing length of the hanging roof in the goaf with the advancement of the panel. When the mining distance reaches the limit equilibrium length of the THRS, the roof will break and collapse because of the combined effect of gravity and the overlying rock load (Yang and Liu, 2019; Guo and Yang, 2021; Sun and Zuo, 2021; Wang and Zhu, 2021). Meanwhile, the research indicates that the mining thickness and overburden key layer structure have a significant effect on the height of the caving zone and fracture zone (Palchik, 2015; Ju and Wang, 2019). Mine tremors are frequently induced by the failure of the THRS and the migration of the overburden structure under strong mining. To prevent or avoid tremors and other dynamic hazards, the lows of overburden structure evolution and stress field change are investigated, and effective control techniques are proposed, e.g., deep-hole blasting (Wang and Tu, 2013; Xu and Fu, 2019; Zhang and Hu, 2021a; Zou and Wu, 2022), hydraulic fracturing (He and Dou, 2012; Zou and Jiao, 2021), and material filling in the goaf (Xue et al., 2020).

In this paper, the position and thickness of key layers are identified using key strata theory. In situ monitoring technology and the finite element method are used to simulate the overlying strata movement during coal mining. The evolution characteristics of overburden structure and stress in deep mining are revealed based on surface subsidence monitoring and numerical simulation. We verify the variation law of stress and deformation in the surrounding roadway rock and analyze the stress distribution characteristics of the coal pillar. The research results could provide theoretical guidance for the prevention and control of mining-induced dynamic hazards in deep coal mines.

2 Engineering background

The coal seam of the Dongtan Coal Mine is very thick and has a deep burial, which is typical of a deep mine. The No.6 mining area is located in the south of the Dongtan mine field (see Figure 1). All mining activities are presently carried out at the first level (−660 m). The main mining seam is

the 3upper coal with a thickness of 0.50–5.40 m. The 3.5 m narrow coal pillars are set between panels. The panels 03/63, 04/63, and 05/63 in the No.6 mining area have completed extraction, and the sequence is 04/63⇢ 05/63⇢ 03/63. Up to 27 March 2021, panel 06/63 has been mined for 630.05 m.

The tectonic of the No.6 mining area is relatively simple: developing sublevel wide and gentle folds, with anticline and syncline distribution among them. Few faults have developed in the mine area. Therefore, the influence of the fault could be ignored in the activity of overlying rock during coal mining. The maximum horizontal principal stress in this area is 24.96–27.12 MPa with the direction of SE 30.00°–31.07°, which is 1.44–1.72 times larger than the vertical stress. We drilled holes from the ground and obtained rock samples of different rock strata. Through the experimental tests, the mechanical parameters of the different rock strata were obtained, as shown in Table 1. The immediate roof above the 3upper coal seam is dark-gray siltstone with an average thickness of 4.54 m and a tensile strength of 7.57 MPa. The main roof is gray-white medium sandstone, the thickness and tensile strength of which are 30.87 m and 8.61 MPa, respectively. Multiple extremely thick and hard sandstone strata are formed above the coal seam and play a dominant role in controlling the evolution of overburden structure.

3 Evolution characteristics of the overburden structure

3.1 Mechanical model of the overburden structure

With the mining of coal seam, the weak direct roof stratum collapses. The hard rock stratum above it deforms, forming a suspended structure. When the initial fracture of the thick and hard rock stratum occurs, the overburden structure changes from the fixed-end beam model to the cantilever beam model (Liu and Li, 2017; Page and Li, 2019; He and Xie, 2021). The overlying strata failure and horizontal stress transfer processes will be repeated during subsequent mining.

(1) Mechanical model of the fixed-end beam

In the initial extraction stage of the coal seam, the mechanical model of the overlying rock fixed-end beam is shown in Figure 2. The maximum tensile stress in the cross-section of the fixed-end beam is located at the position where the section bending moment is the largest and away from the neutral axis of the section. When the tensile stress in the section exceeds the allowable tensile strength of the rock, tensile damage occurs in the overlying rock strata.
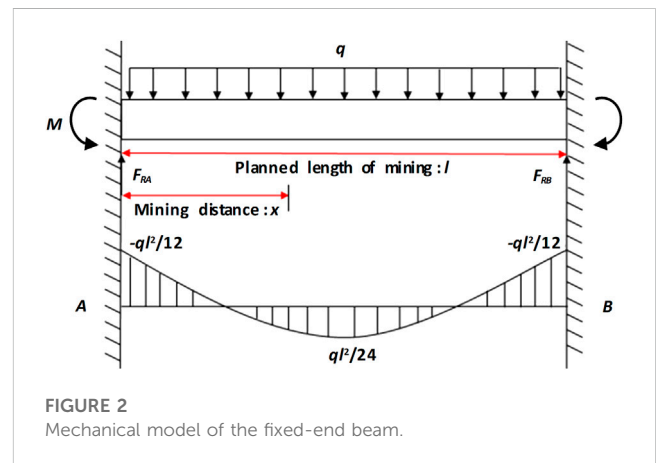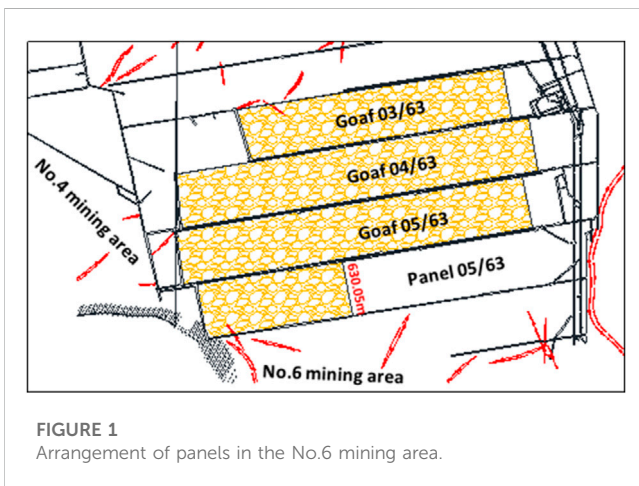
(2) Mechanical model of the cantilever beam

The overburden structure forms the mechanical model of the cantilever beam after the initial fracture occurs (see Figure 3). The cantilever beam breaks and collapses, and the periodic pressure phenomenon appears at the working face when the excavation length achieves the periodic collapse step.

The overlying load is transferred to the unbroken rock when the initial fracture happens at the main roof. Most energy is accumulated in the key layer as the dominant support stratum, which releases a

TABLE 1 Main physical and mechanical parameters of the rock.

Number	Lithology	Key layer	Thickness/m	Compressive strength/MPa	Elastic modulus/GPa	Poisson's ratio
1	Soil		123.08	-	-	-
2	Siltstone		115.66	85.60	21.01	0.29
3	Fine sandstone		21.06	68.35	20.66	0.26
4	Medium sandstone		24.66	50.97	12.45	0.22
5	Fine sandstone		54.17	68.35	20.66	0.26
6	Fine sandstone	Key layer 3	219.22	72.35	19.29	0.21
7	Fine sandstone	Key layer 2	51.29	78.87	15.52	0.16
8	Fine sandstone		12.98	33.34	19.34	0.25
9	Mudstone		8.65	-	-	-
10	Fine sandstone		13.38	46.76	9.85	0.30
11	Medium sandstone		5.50	103.01	30.13	0.27
12	Sandy mudstone		3.08	54.87	13.80	0.26
13	Medium sandstone	Key layer 1	30.87	90.25	36.63	0.23
14	Claystone		1.10	28.44	15.00	0.33
15	Siltstone		1.69	74.88	24.23	0.25
16	Medium sandstone		0.72	106.58	43.35	0.24
17	Siltstone		5.73	107.14	50.89	0.26
18	3upper coal		5.39	-	-	-

FIGURE 1
Arrangement of panels in the No.6 mining area.

FIGURE 2
Mechanical model of the fixed-end beam.

large amount of elastic energy to induce the rock burst or mine tremor (Jiang and Qu, 2013; Yu and Zuo, 2022). Based on key strata theory, the overlying rock strata above the 3upper coal seam are divided into three key layers: key layer 1, a medium sandstone layer with a thickness of 30.9 m, which is 9.2 m above the coal seam; key layer 2: a fine sandstone layer with a thickness of 51.3 m, which is 83.7 m above the coal seam; and key layer 3, a fine sandstone layer with a thickness of 219.2 m, which is 135.0 m above the coal seam.

Because of the low tensile strength of the rock, cracks are generated and expanded at the end of the fixed-end beam under tensile stress and eventually fracture and break through the entire

main roof. The initial fracturing span L of key layers is calculated by the following (Wang and Zhang, 2016; Yang and Liu, 2019):

$$L = h\sqrt{\frac{2Rt}{q}} \tag{1}$$

$$q = \frac{E_1 H_1^3 (\gamma_1 H_1 + \gamma_2 H_2 + \cdots + \gamma_n H_n)}{E_1 H_1^3 + E_2 H_2^3 + \cdots + E_n H_n^3} \tag{2}$$

Where q is the overlying load of the rock stratum, R_t is the tensile strength of the rock, and E, H, and γ are the elastic modulus, thickness, and volumetric weight of the rock strata, respectively.
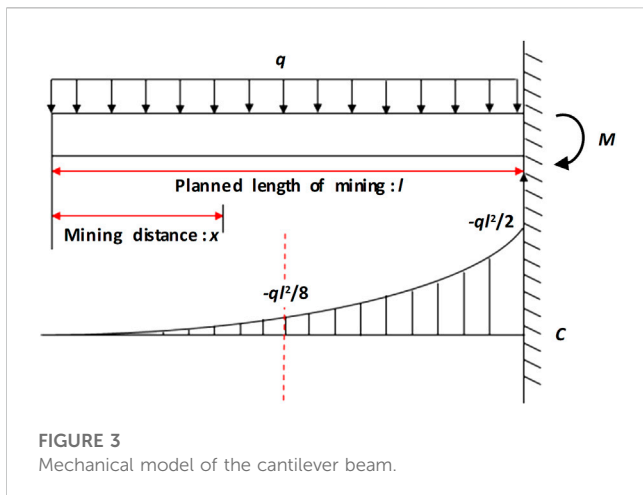
FIGURE 3
Mechanical model of the cantilever beam.

The results show that the initial fracturing spans of key layers 1, 2, and 3 were 95.3, 167.9, and 403.8 m, respectively. According to microseismic monitoring, the first large-energy mine tremor was triggered and located in key layer 1 when panel 06/63 advanced 93.7 5 m. The mine seismic activity occurred in key layer 2 when the panel advanced 150.75 m. The calculation result of the initial fracturing span of the key layer above the coal seam is basically consistent with the actual situation.

3.2 Evolution law of the overburden structure

The overburden structure is gradually developed from the preliminary vertical "O-X" type to the "O" type with continuous mining through the previous investigation of the evolution law of the overburden spatial structure (Dou and He, 2012; Guo and Cao, 2021; Ma and Yuvan, 2021). The formation of stress concentration in front of the working face is likely to cause a rock burst as the overlying load is transferred to the coal mass (Li and Wang, 2016; Yang and Liu, 2019). As shown in Figure 4, strong mine earthquakes occur frequently within the first square of the single goaf in each working face, forming the "O" overburden spatial structure. The SOS microseismic monitoring system is used in this paper to monitor and locate the mine earthquake events. It could realize long-distance (maximum 10 km), real-time, dynamic, and automatic monitoring of mine earthquake signals, including rock bursts, and provides the complete waveform of mine earthquake signals. The system monitors the vibration energy of more than 100 J and the frequency of 0.1–600 Hz vibration. The system has high positioning accuracy by correcting the propagation speed of vibration in the rock stratum.

The goaf below the sandstone strata is filled with fractured rock blocks during the mining of the 3upper coal seam. It causes a little accumulated settlement on the surface without sufficient movement since the movement space is small (Ma and Li, 2008; Xue et al., 2020). The large thickness and high level of the key layer lead to a small opening angle resulting from the break and fracture. In the early stage of mining, the structure of the overlying rock strata fracture in panel 04/63 is the vertical "O-X" type, forming an "O" type overburden structure in the first square of the single goaf. With the increase of the advance length, the overburden structure is gradually converted into the transverse "O-X" type (Dou and He, 2012; Yang and Liu, 2019). It is difficult to isolate the connection between goafs by narrow coal pillars (Yu and Zhang, 2016; Wang and Zhu, 2021; Song and Lu, 2022), which form the transverse "O-X" structure within the first square of the double goafs. The overlying rock strata are periodically fractured by subsequent extraction, which is in a half "O-X" break shape. The transverse "O-X" overburden structure is created in the first square of the three goafs when panel 03/63 is mined.

In Figure 5, the width of the panels is significantly larger than the coal pillar. The overlying load is delivered to the coal pillar and coal
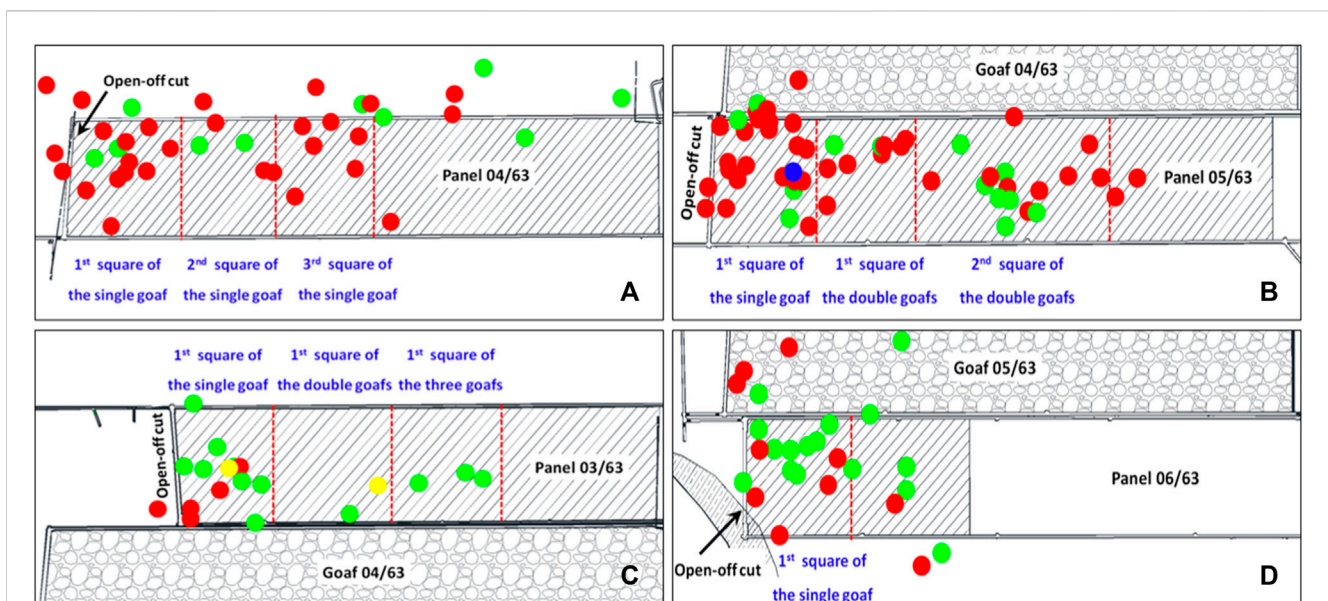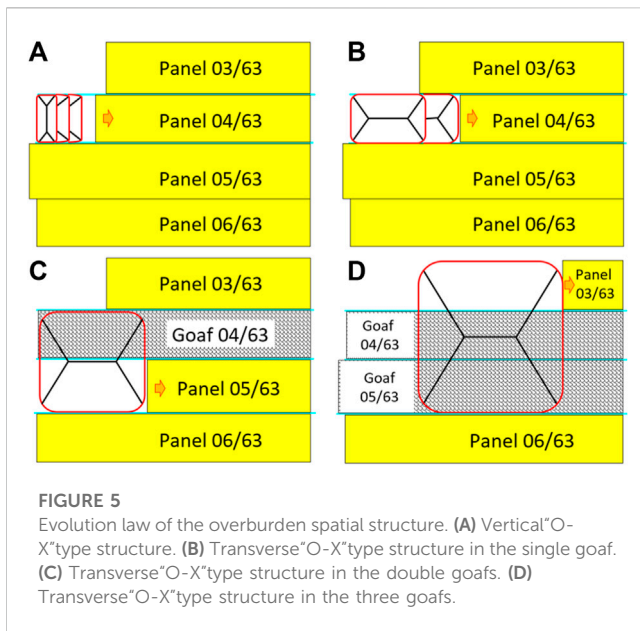

FIGURE 4
Distribution characteristics of strong mine tremors ($\bullet$: E $>10^4$ J; $\bullet$: E $>10^5$ J; $\bullet$: E $>10^6$ J; $\bullet$: E $>10^7$ J). **(A)** Strong mine tremor events at panel 04/63. **(B)** Strong mine tremor events at panel 05/63. **(C)** Strong mine tremor events at panel 03/63. **(D)** Strong mine tremor events at panel 06/63.

FIGURE 5
Evolution law of the overburden spatial structure. **(A)** Vertical"O-X"type structure. **(B)** Transverse"O-X"type structure in the single goaf. **(C)** Transverse"O-X"type structure in the double goafs. **(D)** Transverse"O-X"type structure in the three goafs.

body with the length of retrieval, which will result in compression and deformation of the coal pillar. Under the increasing length of the overhanging roof, the narrow coal pillar could hardly support the overlying load, leading to failure and instability and subsequent rock burst events. The coal pillar is reserved between panels of deep mines, which is used to isolate the goaf and maintain the stability of the surrounding roadway rock (Yu and Zhang, 2016; Wu and Bai, 2019; Xia and Yao, 2021).

4 Evolution laws of overburden stress and deformation

4.1 Numerical modeling

FEM was applied to establish the three-dimensional numerical simulation model of the No.6 mining area in the Dongtan Coal Mine. The extraction process was analyzed to reveal the evolution laws of overburden stress and deformation from deep mining. As shown in Figure 6, the geometry size of the model was 2,000 m (length) × 1,680 m (width) × 286 m (height). The horizontal displacement and degree of freedom constraints were set on the periphery, and vertical displacement and degree of freedom constraints were applied to the bottom.

To reveal the overburden stress and deformation law of deep mining, the mining process of panel 06/63 was studied. The excavated coal body was removed using the model change function. Application of gravity stress and initial geo-stress to achieve ground stress balance *in situ* stress field balance. Combined with the laboratory tests, the physical and mechanical parameters of the rock are shown in Table 1.

4.2 Evolution laws of overburden stress and deformation

Figures 7, 8 show the distribution of the maximum principal stress at the advance of 550.20 m on panel 06/63. The maximum principal stress is first concentrated in the hard interlayer between the coal seam and key layer 1. The elastic modulus of the 9.2 m thick interlayer is as high as 51 GPa, which is higher than thick and hard sandstone strata. Under the effect of mining bearing pressure, the coal body in front of the working face will be deformed to a certain extent. At the same time, the distribution of existing goafs will inevitably have a significant impact on the spatial distribution of stress, displacement, and energy accumulation in the panel (Wang and Duan, 2017; Zhang and Hu, 2021).

As of 9 April 2021, the surface settlement of panel 06/63 is monitored and the maximum cumulative surface settlement is 1,803.7 mm (see Figure 9). The offset of the cumulative settlement maximum point in the direction of mining increases gradually with the continuous advancement of the panel. This indicates that the continuous advance of the panel has caused the distribution range of the "Three Zones" of the overburden rock to extend and shift in the upper layer. The movement of the overlying
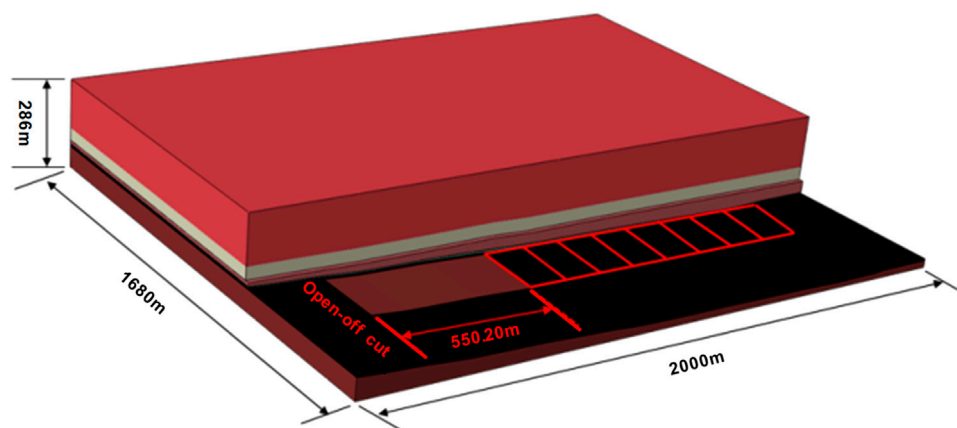

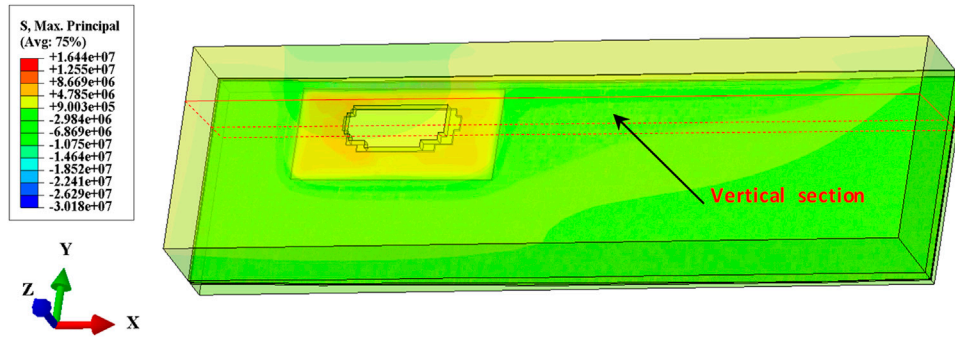**FIGURE 6**
The three dimensions of the simulation model.

FIGURE 7
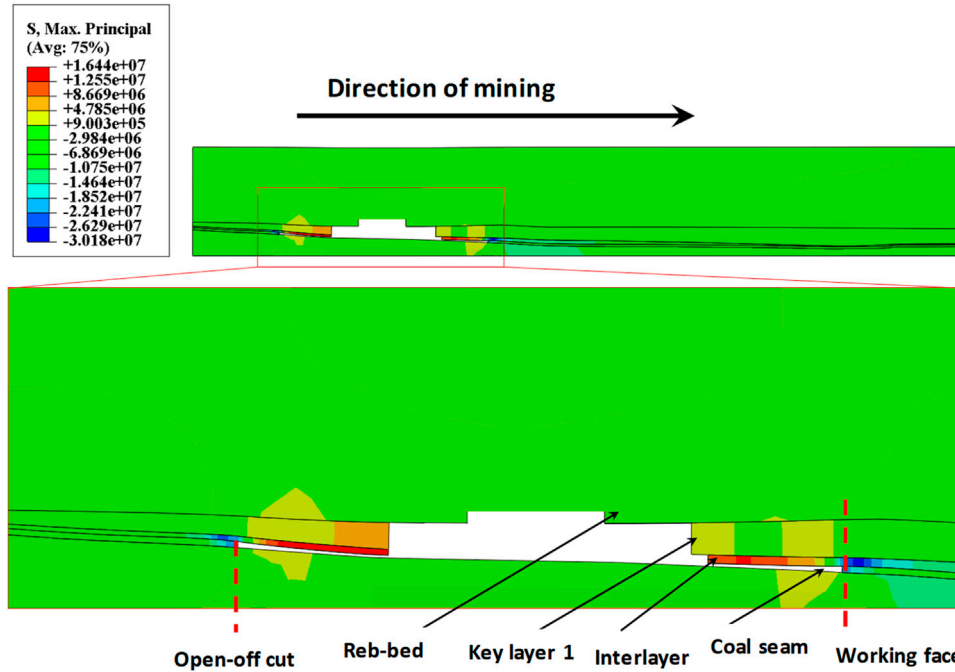Distribution of the maximum principal stress at the advance of 550.20 m on panel 06/63.

FIGURE 8
Vertical section distribution of the maximum principal stress.

key layer significantly controls surface subsidence, increasing with layer-by-layer upward fracture migration and surface subsidence activity (Jiang and Wu, 2019; Liu and Li, 2019; Wang and Jiang, 2019). Surface subsidence enters the peak state until the key layer stops rotating in the forward direction and starts rotating in the reverse direction.

The surface subsidence is minor at the early stage of mining, and then large subsidence occurs near the location of the open-off cut. The surface subsidence reaches the maximum at the position of approximately 1/5 mining length from the open-off cut. The end of the active period of surface subsidence depends on the stabilization of the most upward key layer movement. The final

shape of surface subsidence is directly controlled by the movement state of key layers (Chen and Chen, 2019; Jiang and Wu, 2019; Xue and Xu, 2020).

As shown in Figure 10, the deformation displacement near the direction of the 05/63 goaf is the largest, leaving the direction of the goaf displacement gradually decreasing. During the mining process of panel 06/63, the roof of the back goaf collapses and forms an overburden spatial structure together with one side of the goaf. It is one of the major reasons for the asymmetric deformation of the panel surrounding rock. In addition, it will cause an increase in advancing abutment pressure on the working face causing strong strata behaviors.
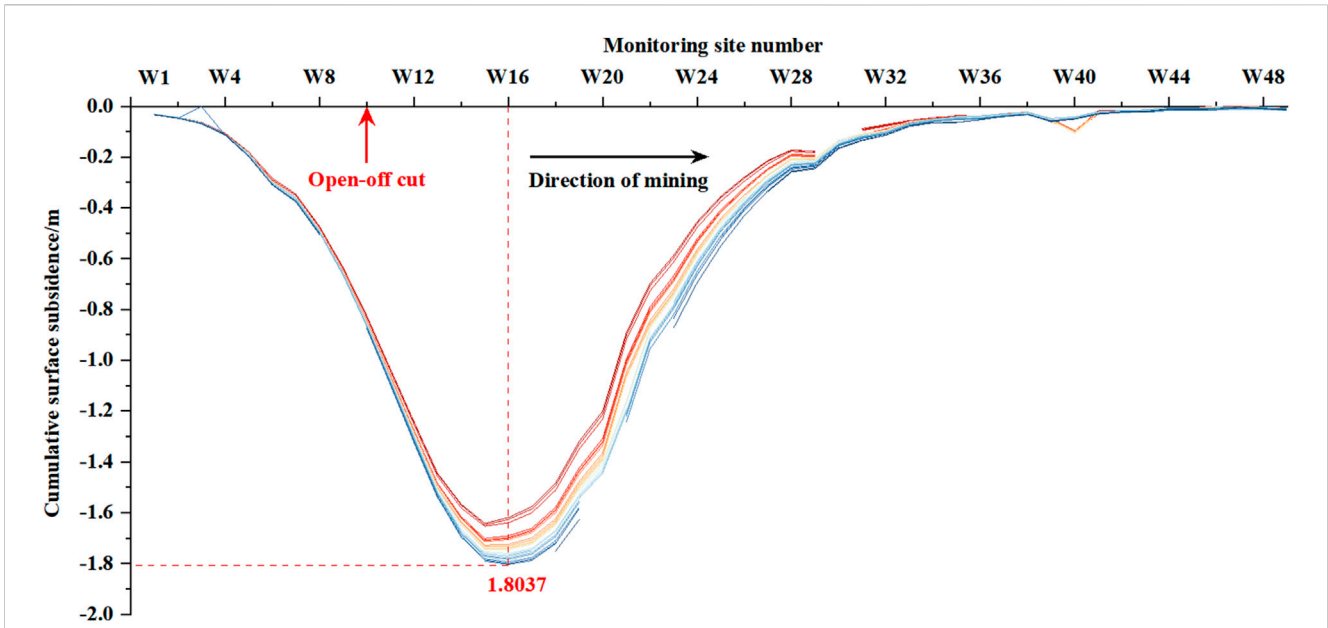
FIGURE 9
The surface subsidence curve of panel 06/63 (monitoring stations: W1−W49).
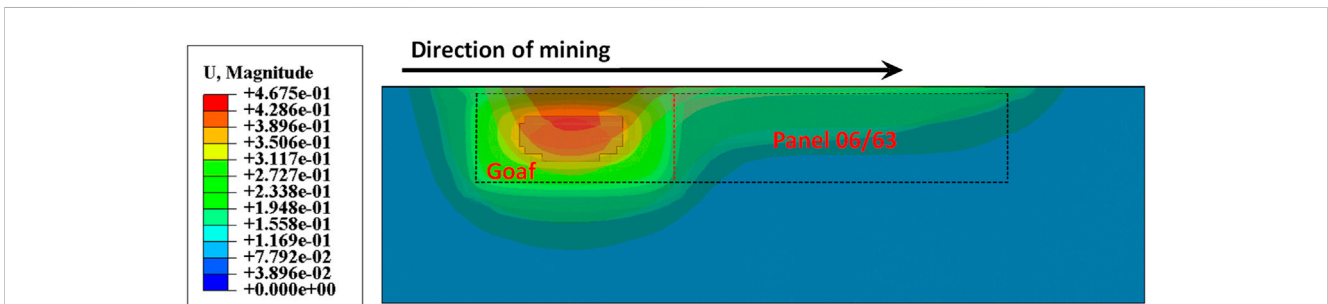

FIGURE 10
Cloud diagram of the surrounding rock deformation distribution at panel 06/63.
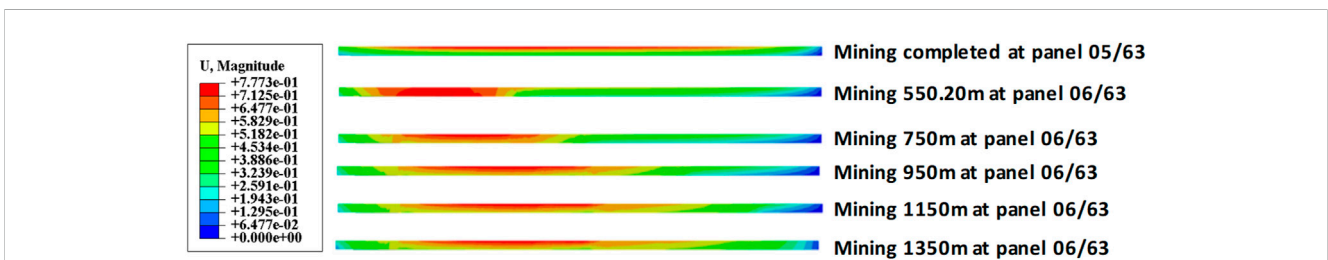

FIGURE 11
Prediction of coal pillar deformation on the side of the auxiliary transport gateway at panel 06/63.

4.3 Evolution law of coal pillar stress

Combined with the cloud diagram of coal pillar deformation, the coal pillar at the auxiliary transport gateway has generated the corresponding deformation and the deformation degree is large on the side near the goaf before panel 06/63 advances. With the breaking and collapse of the overlying rock strata in the goaf, the stress concentration zone is formed in the narrow coal pillar within the goaf under the action of the overlying load. As shown in Figure 11, the
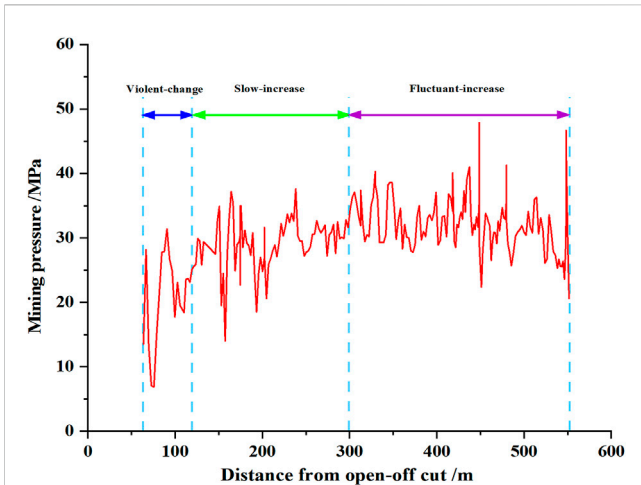
FIGURE 12
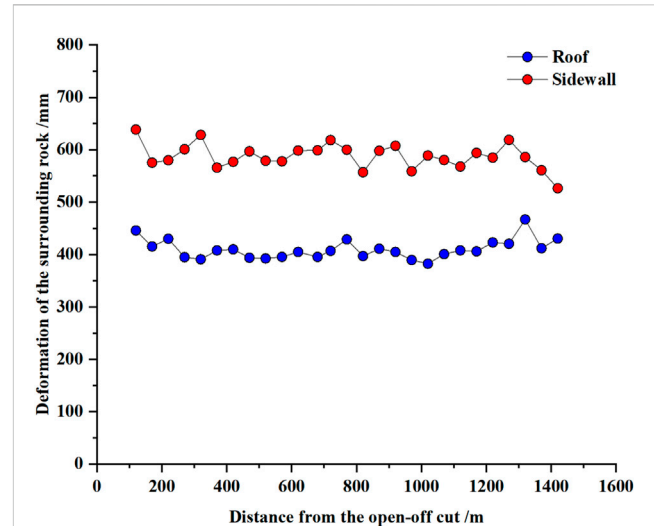The relationship between mining pressure and the extraction distance of the working face.

FIGURE 14
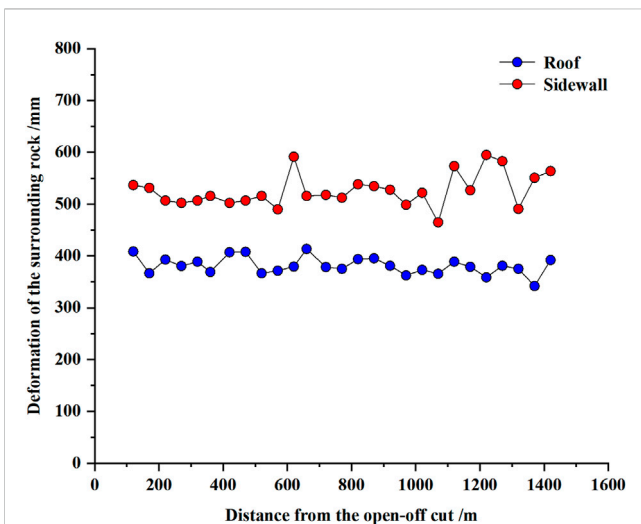The deformation of the sidewall and roof of the conveyor gateway.

FIGURE 13
The deformation of the sidewall and roof of the auxiliary transport gateway.

position of stress concentration has a relatively high degree of deformation. Because of the expanding range of the goaf, the coal pillar deformation zone develops forward but the volume of deformation decreases.

The stress in the coal pillar is greatly concentrated under the self-weight stress, tectonic stress, roadway excavation, and pressure relief transfer stress. When the concentration stress exceeds the bearing capacity of the coal pillar, impact instability occurs in the middle elastic core of the coal pillar (Zhu and Chen, 2019; Zhang and Zhao, 2022). The calculation results show that the stress of the coal pillar after excavation has exceeded its bearing capacity, which has lost the role of maintaining the stability of the roadway surrounding rock. The plane distribution of mine tremors verifies the above idea that there are seismic mine events in the 05/63 goaf during the mining process of panel 06/63.

5 Evolution laws of surrounding rock stress and deformation

5.1 Evolution law of surrounding rock stress at the working face

The dynamic evolution of surrounding rock stress at the working face during the advancement of panel 06/63 is shown in Figure 12. During the first caving and weighting, the YHY60(B) type support resistance recorder is used to monitor the changes in mining pressure at the working face. Monitoring shows that the initial *in situ* stress of overburden is approximately 30 MPa. In the range of 60–120 m from the open-off cut, the overlying rock strata instantly break and collapse, showing a significant decrease and increase in the surrounding rock stress of the working face. When the panel advances to 300 m, the overlying load re-acts at the monitoring point with the overburden strata fracture, collapse, and compaction at 120–300 m from the open-off cut. The stress of overburden in the working face gradually returns to the initial stress. The surrounding rock stress fluctuates and appears to be weakly increasing, basically staying at approximately 30 MPa in the subsequent range.

Breaking and collapsing of the overlying rock strata is a dynamic motion process. The caving zone of the overburden expands and moves forward with the mining of the panel. The evolution process of surrounding rock stress in the working face is divided into slow-increase and fluctuant-increase stages. The instantaneous fracture of the rock strata leads to the abrupt release of accumulated energy, which induces a rapid decrease in overburden stress at the stage of violent change. At the same time, the falling rock is in the shape of giant blocks, and the phenomenon of strata behaviors is obvious (Wang and Bian, 2019; Zou and Hu, 2022). At the slow-increase stage, the main roof fractures and falls again, and the collapsed rock blocks act on the hydraulic support based on the previously formed gangue, causing

the surrounding rock stress to rise slowly. At the fluctuant-increase stage, the surrounding rock stress is continuously redistributed under the coal seam excavation, which experiences strong fluctuations and weak increases.

5.2 Evolution law of the surrounding rock deformation

To investigate the deformation of the surrounding rock of the roadway in panel 06/63, monitoring points were arranged in the conveyor gateway and auxiliary transport gateway to monitor the deformation of the sidewall and roof of the roadway. As shown in Figures 13, 14, the monitoring results indicate that the evolution process of the surrounding rock deformation in the sidewall and roof of the conveyor gateway and auxiliary transport gateway is basically the same.

The overall trend of roof deformation is increasing at first and then decreasing, and the maximum deformation is almost at the center of the roof. The sidewall deformations of the auxiliary transport gateway and conveyor gateway are maintained at approximately 500 mm and 600 mm, respectively. The difference in the sidewall deformation of roadways is that the auxiliary transport gateway is close to the 05/63 goaf. Both sides of the conveyor gateway are coal bodies causing local stress concentration and energy accumulation, which results in larger displacements for energy dissipation and stress release.

6 Conclusion

This paper investigated the evolution of overburden structure and stress in the mining of the deep mine based on field monitoring and numerical simulation. The three-dimensional numerical model was established by the finite element method and the evolution law of surrounding rock stress and coal pillar stress was investigated. The main conclusions are as follows.

(1) The movement of the overburden strata conforms to the fixed-end beam model at the initial stage of excavation and is converted to the cantilever-beam model after the initial fracture. According to the characteristics of mine earthquakes, the overburden structure shows the "O-X" type spatial structure evolution and the connection between adjacent goafs is not isolated.

(2) Based on key strata theory, three key layers are determined, which play the dominant role in controlling overlying strata migration. The initial fracturing spans of key layers based on theoretical calculations are 95.3 m, 167.9 m, and 403.8 m, respectively. The final shape of surface subsidence in deep mining is significantly correlated with the movement state of key layers.

(3) The overlying rock stress concentration occurs mainly in the immediate roof and key layers. The narrow coal pillar makes it difficult to isolate the connection between the goaf and the panel. The numerical simulation revealed that the coal pillar has lost its role in maintaining the stability of the overlying strata. The adjacent goaf inevitably has a great impact on the spatial distribution of stress, deformation, and energy accumulation in the overburden.

(4) The evolution process of surrounding rock stress at the working face is categorized into three stages: violent change, slow increase, and fluctuant increase. Strong strata movement behaviors are caused by the fracture and collapse of key layers in the early mining stage of the panel. The deformation law of surrounding rock mass in the sidewall and roof of the conveyor gateway and auxiliary transport gateway is basically the same.

Data availability statement

The raw data supporting the conclusion of this article will be made available by the authors, without undue reservation.

Author contributions

JZ: Investigation, Writing–original draft, Funding acquisition. MW: Investigation, Funding acquisition, Writing–review and editing. LB: Methodology, Writing–review and editing. CY: Formal Analysis, Writing–review and editing.

Conflict of interest

The authors declare that the research was conducted in the absence of any commercial or financial relationships that could be construed as a potential conflict of interest.

Publisher's note

All claims expressed in this article are solely those of the authors and do not necessarily represent those of their affiliated organizations, or those of the publisher, the editors and the reviewers. Any product that may be evaluated in this article, or claim that may be made by its manufacturer, is not guaranteed or endorsed by the publisher.

References

Chen, S. J., Chen, B., Yin, D., and Guo, W. (2019). Characteristics of discontinuous surface deformation due to mining in hard, thick bedrock: a case study. *Geotech. Geol. Eng.* 37, 2639–2645. doi:10.1007/s10706-018-00783-z

Dou, L. M., and He, H. (2012). Study of OX-F-T spatial structure evolution of overlying strata in coal mines. *Chin. J. Rock Mech. Eng.* 31 (3), 453–460. doi:10.3969/j.issn.1000-6915.2012.03.003

Dou, L. M., He, X. Q., He, H., He, J., and Fan, J. (2014). Spatial structure evolution of overlying strata and inducing mechanism of rockburst in coal mine. *Trans. NonferrousMetals Soc. China* 24 (4), 1255–1261. doi:10.1016/s1003-6326(14)63187-3

Guo, G. C., and Yang, Y. K. (2021). The study of key stratum location and characteristics on the mining of extremely thick coal seam under goaf. *Adv. Civ. Eng.* 2021, 1–9. doi:10.1155/2021/8833822

Guo, H., Yuan, L., Shen, B., Qu, Q., and Xue, J. (2012). Mining-induced strata stress changes, fractures and gas flow dynamics in multi-seam longwall mining. *Int. J. Rock Mech. Min. Sci.* 54, 129–139. doi:10.1016/j.ijrmms.2012.05.023

Guo, W. H., Cao, A. Y., Xue, C., Hu, Y., Wang, S., and Zhao, Q. (2021). Mechanism and evolution control of wide coal pillar bursts in multithick key strata. *Adv. Civ. Eng.* 2021, 1–14. doi:10.1155/2021/4696619

Hatherly, P. (2013). Overview on the application of geophysics in coal mining. *Int. J. Coal Geol.* 114, 74–84. doi:10.1016/j.coal.2013.02.006

He, H., Dou, L. M., Cao, A., and Fan, J. (2015). Mechanisms of mining seismicity under large scale exploitation with multikey strata. *Shock Vib.* 2015, 1–9. doi:10.1155/2015/313069

He, H., Dou, L. M., Fan, J., Du, T., and Sun, X. (2012). Deep-hole directional fracturing of thick hard roof for rockburst prevention. *Tunn. Undergr. Sp. Tech.* 32, 34–43. doi:10.1016/j.tust.2012.05.002

He, Z. Q., Xie, H. P., Gao, M., Chen, L., Yu, B., Hu, Y., et al. (2020). Design and verification of a deep rock corer with retaining the *in situ* temperature. *Adv. Civ. Eng.* 2020, 1–13. doi:10.1155/2020/8894286

He, Z. Q., Xie, H. P., Gao, M., Deng, G., and Peng, G. (2021). The fracturing models of hard roofs and spatiotemporal law of mining-induced stress in a top coal caving face with an extra-thick coal seam. *Geomech. Geophys Geo* 7, 2. doi:10.1007/s40948-020-00202-9

Jian, S. (2017). Mechanics criterion and factors affecting overburden stability in solid dense filling mining. *Int. J. Min. Sci. Technol.* 27 (3), 407–413. doi:10.1016/j.ijmst.2017.03.010

Jiang, F. X., Qu, X. C., et al. (2013). Case study on the mine earthquake caused by hard rock fracture in Baodian Coal Mine. *J. China Coal Soc.* 38 (S2), 319–324. doi:10.13225/j.cnki.jccs.2013.s2.032

Jiang, L. S., Wu, Q. S., Wang, P., Xue, Y., Kong, P., et al. (2019). Fracture failure analysis of hard and thick key layer and its dynamic response characteristics. *Eng. Fail Anal.* 98, 118–130. doi:10.1016/j.engfailanal.2019.01.008

Jiao, Y. Y., Wu, K. B., Zou, J., Zheng, F., Zhang, X., Wang, C., et al. (2021). On the strong earthquakes induced by deep coal mining under thick strata-a case study. *Geomech. Geophys Geo* 7, 97. doi:10.1007/s40948-021-00301-1

Ju, F., Xiao, M., He, Z., Ning, P., and Huang, P. (2018). Study on fracture and stress evolution characteristics of ultra-thick hard sandstone roof in the fully mechanized mining face with large mining height: a case study of xiaojihan coal mine in western China. *Adv. Civ. Eng.* 2018, 1–12. doi:10.1155/2018/5474165

Ju, J. F., and Xu, J. L. (2013). Structural characteristics of key strata and strata behaviour of a fully mechanized longwall face with 7.0 m height chocks. *Int. J. Rock Mech. Min. Sci.* 58, 46–54. doi:10.1016/j.ijrmms.2012.09.006

Ju, Y., Wang, Y. L., Su, C., Zhang, D., and Ren, Z. (2019). Numerical analysis of the dynamic evolution of mining-induced stresses and fractures in multilayered rock strata using continuum-based discrete element methods. *Int. J. Rock Mech. Min. Sci.* 113, 191–210. doi:10.1016/j.ijrmms.2018.11.014

Kuang, T. J., Li, Z., Zhu, W., Xie, J., Ju, J., Liu, J., et al. (2019). The impact of key strata movement on ground pressure behaviour in the Datong coalfield. *Int. J. Rock Mech. Min. Sci.* 119, 193–204. doi:10.1016/j.ijrmms.2019.04.010

Li, X. L., Wang, E. Y., Li, Z., Liu, Z., Song, D., and Qiu, L. (2016). Rock burst monitoring by integrated microseismic and electromagnetic radiation methods. *Rock Mech. Rock Eng.* 49, 4393–4406. doi:10.1007/s00603-016-1037-6

Liu, C., Li, H. M., and Mitri, H. (2019). Effect of strata conditions on shield pressure and surface subsidence at a longwall top coal caving working face. *Rock Mech. Rock Eng.* 52, 1523–1537. doi:10.1007/s00603-018-1601-3

Liu, C., Li, H. M., Mitri, H., Jiang, D., and Feng, J. (2017). Voussoir beam model for lower strong roof strata movement in longwall mining - case study. *J. Rock Mech. Geotech. Eng.* 9 (6), 1171–1176. doi:10.1016/j.jrmge.2017.07.002

Lu, Y. Y., Gong, T., Xia, B., Yu, B., and Huang, F. (2019). Target stratum determination of surface hydraulic fracturing for far-field hard roof control in underground extra-thick coal extraction: a case study. *Rock Mech. Rock Eng.* 52, 2725–2740. doi:10.1007/s00603-018-1616-9

Ma, C. D., Li, X. B., Hu, B. n., Chen, F., and Xu, J. c. (2008). Settlement behavior of coal mine waste in different surrounding rock conditions. *J. Cent. South Univ.* 15, 350–355. doi:10.1007/s11771-008-0066-z

Ma, K., Yuan, F. Z., Wang, H., Zhang, Z., Sun, X., Peng, Y., et al. (2021). Fracture mechanism of roof key strata in Dongjiahe coal mine using microseismic moment tensor. *Geomatics Nat. Hazards Risk* 12 (1), 1467–1487. doi:10.1080/19475705.2021.1933615

Ma, X., Westman, E., Counter, D., Malek, F., and Slaker, B. (2020). Passive seismic imaging of stress evolution with mining-induced seismicity at hard-rock deep mines. *Rock Mech. Rock Eng.* 53, 2789–2804. doi:10.1007/s00603-020-02076-5

Mondal, D., Roy, P. N. S., and Kumar, M. (2020). Monitoring the strata behavior in the Destressed Zone of a shallow Indian longwall panel with hard sandstone cover using Mine-Microseismicity and Borehole Televiewer data. *Eng. Geol.* 271, 105593. doi:10.1016/j.enggeo.2020.105593

Mu, Z. L., Liu, G. J., Yang, J., Zhao, Q., Javed, A., Gong, S., et al. (2019). Theoretical and numerical investigations of floor dynamic rupture: a case study in Zhaolou Coal Mine, China. *Saf. Sci.* 114, 1–11. doi:10.1016/j.ssci.2018.12.016

Page, P., Li, L., Yang, P., and Simon, R. (2019). Numerical investigation of the stability of a base-exposed sill mat made of cemented backfill. *Int. J. Rock Mech. Min. Sci.* 114, 195–207. doi:10.1016/j.ijrmms.2018.10.008

Palchik, V. (2015). Bulking factors and extents of caved zones in weathered overburden of shallow abandoned underground workings. *Int. J. Rock Mech. Min. Sci.* 79, 227–240. doi:10.1016/j.ijrmms.2015.07.005

Qian, M. G., Miao, X. X., et al. (2000). *Key strata theory in ground control*. China.

Song, C. H., Lu, C. P., Zhang, X. F., Wang, C., Xie, H. D., Yan, X. Y., et al. (2022). Moment tensor inversion and stress evolution of coal pillar failure mechanism. *Rock Mech. Rock Eng.* 55, 2371–2383. doi:10.1007/s00603-022-02783-1

Sun, Y. J., Zuo, J. P., Karakus, M., Liu, L., Zhou, H., and Yu, M. (2021). A new theoretical method to predict strata movement and surface subsidence due to inclined coal seam mining. *Rock Mech. Rock Eng.* 54, 2723–2740. doi:10.1007/s00603-021-02424-z

Wang, F., Jiang, B. Y., Chen, S., and Ren, M. (2019). Surface collapse control under thick unconsolidated layers by backfilling strip mining in coal mines. *Int. J. Rock Mech. Min. Sci.* 113, 268–277. doi:10.1016/j.ijrmms.2018.11.006

Wang, F. T., Duan, C. H., Tu, S., Liang, N., and Bai, Q. (2017). Hydraulic support crushed mechanism for the shallow seam mining face under the roadway pillars of room mining goaf. *Int. J. Min. Sci. Technol.* 27 (5), 853–860. doi:10.1016/j.ijmst.2017.07.013

Wang, F. T., Ma, Q., Li, G., Wu, C., and Guo, G. (2018). Overlying strata movement laws induced by longwall mining of deep buried coal seam with superhigh-water material backfilling technology. *Adv. Civ. Eng.* 2018, 1–10. doi:10.1155/2018/4306239

Wang, F. T., Tu, S. H., Yuan, Y., Feng, Y., and Chen, F. (2013). Deep-hole pre-split blasting mechanism and its application for controlled roof caving in shallow depth seams. *Int. J. Rock Mech. Min. Sci.* 64, 112–121. doi:10.1016/j.ijrmms.2013.08.026

Wang, H. S., Shuang, H. Q., Li, L., and Xiao, S. S. (2021). The stability factors' sensitivity analysis of key rock B and its engineering application of gob-side entry driving in fully-mechanized caving faces. *Adv. Civ. Eng.* 2021, 1–11. doi:10.1155/2021/9963450

Wang, S. L., Zhang, K. Z., et al. (2016). The fracture and rockburst laws of high-position hard and extremely thick red beds. *J. Min. Saf. Eng.* 33 (6), 1116–1122. doi:10.13545/j.cnki.jmse.2016.06.023

Wang, S. L., Zhu, G. L., et al. (2021). Study on characteristics of mining earthquake in multicoal seam mining under thick and hard strata in high position. *Shock Vib.*, 6675089. doi:10.1155/2021/6675089

Wang, Z. C., and Bian, W. R. (2019). Analysis of pressure relief effect on the protective layer of hard and extra-thickness coal seam mining. *Geotech. Geol. Eng.* 37, 163–172. doi:10.1007/s10706-018-0600-1

Wu, K. B., Zou, J. P., Jiao, Y. Y., He, S., and Wang, G. (2023). Insight and effectiveness of working-face-deep-hole-blasting for prevention of strong seismicity induced by deep coal mining. *Rock Mech. Rock Eng.*, doi:10.1007/s00603-023-03516-8

Wu, L. X., Qian, M. G., and Wang, J. Z. (1997). The influence of a thick hard rock stratum on underground mining subsidence. *Int. J. Rock Mech. Min. Sci.* 34 (2), 341–344. doi:10.1016/S0148-9062(96)00028-9

Wu, W. D., Bai, J. B., Wang, X. y., Yan, S., and Wu, S. x. (2019). Numerical study of failure mechanisms and control techniques for a gob-side yield pillar in the sijiazhuang coal mine, China. *Rock Mech. Rock Eng.* 52, 1231–1245. doi:10.1007/s00603-018-1654-3

Xia, Z., Yao, Q. L., Meng, G., Xu, Q., Tang, C., Zhu, L., et al. (2021). Numerical study of stability of mining roadways with 6.0-m section coal pillars under influence of repeated mining. *Int. J. Rock Mech. Min. Sci.* 138, 104641. doi:10.1016/j.ijrmms.2021.104641

Xie, H. P., Gao, M. Z., Zhang, R., Peng, G., Wang, W., and Li, A. (2019). Study on the mechanical properties and mechanical response of coal mining at 1000 m or deeper. *Rock Mech. Rock Eng.* 52, 1475–1490. doi:10.1007/s00603-018-1509-y

Xie, H. P., Li, C., He, Z., Lu, Y., Zhang, R., et al. (2021). Experimental study on rock mechanical behavior retaining the *in situ* geological conditions at different depths. *Int. J. Rock Mech. Min. Sci.* 138, 104548. doi:10.1016/j.ijrmms.2020.104548

Xu, C., Fu, Q., Cui, X., Wang, K., Zhao, Y., and Cai, Y. (2019). Apparent-depth effects of the dynamic failure of thick hard rock strata on the underlying coal mass during underground mining. *Rock Mech. Rock Eng.* 52, 1565–1576. doi:10.1007/s00603-018-1662-3

Xue, Y. C., Wu, Q. S., and Sun, D. Q. (2020). Numerical investigation on overburden migration behaviors in stope under thick magmatic rocks. *Geomech. Eng.* 22 (4), 349–359. doi:10.12989/gae.2020.22.4.349

Xue, Y. C., Xu, T., Wasantha, P. L. P., Yang, T. h., and Fu, T. f. (2020). Dynamic disaster control of backfill mining under thick magmatic rock in one side goaf: a case study. *J. Cent. South Univ.* 27, 3103–3117. doi:10.1007/s11771-020-4532-6

Yang, Z. Q., Liu, C., Zhu, H., Xie, F., Dou, L., and Chen, J. (2019). Mechanism of rock burst caused by fracture of key strata during irregular working face mining and its prevention methods. *Int. J. Min. Sci. Technol.* 29 (6), 889–897. doi:10.1016/j.ijmst.2018.07.005

Yu, B., Zhang, Z. Y., Kuang, T., and Liu, J. (2016). Stress changes and deformation monitoring of longwall coal pillars located in weak ground. *Rock Mech. Rock Eng.* 49, 3293–3305. doi:10.1007/s00603-016-0970-8

Yu, M. L., Zuo, J. P., Sun, Y., Mi, C., and Li, Z. (2022). Investigation on fracture models and ground pressure distribution of thick hard rock strata including weak interlayer. *Int. J. Min. Sci. Technol.* 32 (1), 137–153. doi:10.1016/j.ijmst.2021.10.009

Zhang, C., Zhao, Y. X., Han, P., and Bai, Q. (2022). Coal pillar failure analysis and instability evaluation methods: a short review and prospect. *Eng. Fail Anal.* 138, 106344. doi:10.1016/j.engfailanal.2022.106344

Zhang, M., Hu, X. L., et al. (2021a). Mechanism and prevention and control of mine earthquake in thick and hard rock strata considering the horizontal stress evolution of stope. *Shock Vib.*, 6680928. doi:10.1155/2021/6680928

Zhang, Q., Zou, J. P., Wang, J., Jiao, Y. Y., and Xu, H. (2023). Mechanism of coal bump induced by joint slipping under static and dynamic stresses in graben structural area. *ACTA Geotech.*, doi:10.1007/s11440-023-01947-9

Zhang, X. Q., Hu, B. L., Zou, J., Liu, C., and Ji, Y. (2021b). Quantitative characterization of overburden rock development pattern in the goaf at different key stratum locations based on DEM. *Adv. Civ. Eng.* 2021, 1–18. doi:10.1155/2021/8011350

Zhou, C., Zhu, S. T., Song, D., Jiang, F., Liu, J., and Li, J. (2022). Study on the mechanism of repeated mining tremor in multiple key layers: a typical case study. *Geotech. Geol. Eng.* 40, 5139–5151. doi:10.1007/s10706-022-02208-4

Zhu, W. B., Chen, L., Zhou, Z., Shen, B., and Xu, Y. (2019). Failure propagation of pillars and roof in a room and pillar mine induced by longwall mining in the lower seam. *Rock Mech. Rock Eng.* 52, 1193–1209. doi:10.1007/s00603-018-1630-y

Zou, J. P., Hu, X. Y., Jiao, Y. Y., Chen, W., Wang, J., Shen, L. W., et al. (2022). Dynamic mechanical behaviors of rock's joints quantified by repeated impact loading experiments with digital imagery. *Rock Mech. Rock Eng.* 55, 7035–7048. doi:10.1007/s00603-022-03004-5

Zou, J. P., Jiao, Y. Y., Tan, F., Lv, J., and Zhang, Q. (2021). Complex hydraulic-fracture-network propagation in a naturally fractured reservoir. *Comput. Geotech.* 135, 104165. doi:10.1016/j.compgeo.2021.104165

Zou, J. P., Wu, K. B., Zhang, X., Zhu, J., Zhou, Z., Zheng, F., et al. (2022). Effective evaluation of deep-hole blasting for controlling strong tremors induced by deep coal mining-A case study. *Int. J. Rock Mech. Min. Sci.* 159, 105211. doi:10.1016/j.ijrmms.2022.105211